Effects of the Disappearance of One Charge on Ultrafast Fluorescence Dynamics of the FMN Binding Protein

Haik Chosrowjan,*,† Seiji Taniguchi,† Noboru Mataga,† Takeshi Nakanishi,‡ Yoshihiro Haruyama,‡ Shuta Sato,‡ Masaya Kitamura,*,‡ and Fumio Tanaka*,§

Institute for Laser Technology, Utsubo-Hommachi 1-8-4, Nishiku, Osaka 550-0004, Japan, Department of Applied Chemistry and Bioengineering, Graduate School of Engineering, Osaka City University, 3-3-138 Sugimoto, Sumiyoshiku, Osaka 558-8585, Japan, and Department of Biochemistry, Center for Excellence in Protein Structure and Function, Faculty of Science, Mahidol University, 272 Rama VI Road, Bangkok, 10400, Thailand

Received: December 23, 2009; Revised Manuscript Received: March 2, 2010

Crystal structures of E13T (Glu13 was replaced by Thr13) and E13Q (Glu13 was replaced by Gln13) FMN binding proteins (FMN-bp) from *Desulfovibrio vulgaris*, strain Miyazaki F, were determined by the X-ray diffraction method. Geometrical factors related to photoinduced electron transfer from Trp32, Tyr35, and Trp106 to the excited isoalloxazine (Iso*) were compared among the three forms of FMN-bp. The rate of ET is considered to be fastest from Trp32 to Iso* in FMN-bp and then from Tyr35 and Trp106. The distances between Iso and Trp32 did not change appreciably (0.705−0.712 nm) among WT, E13T, and E13Q FMN-bps, though the distances between Iso and Tyr35 or Trp106 became a little shorter by ca. 0.01 nm in both mutated FMN-bps. The distances between the residue at 13 and the ET donors or acceptor in the mutated proteins, however, changed markedly, compared to WT. Hydrogen bonding pairs and distances between Iso and surrounding amino acids were not modified when Glu13 was replaced by Thr13 or Gln13. Effects of elimination of ionic charge at Glu13 on the ultrafast fluorescence dynamics in E13T and E13Q were investigated comparing to WT, by means of a fluorescence up-conversion method. Fluorescence lifetimes were $\tau_1 = 107$ fs ($\alpha_1 = 0.86$), $\tau_2 = 475$ fs ($\alpha_2 = 0.12$), and $\tau_3 = 30$ ps ($\alpha_3 = 0.02$) in E13T and $\tau_1 = 134$ fs ($\alpha_1 = 0.85$), $\tau_2 = 746$ fs ($\alpha_2 = 0.12$), and $\tau_3 = 30$ ps ($\alpha_3 = 0.03$) in E13Q, which are compared to the reported lifetimes in WT, $\tau_1 = 168$ fs ($\alpha_1 = 0.95$) and $\tau_2 = 1.4$ ps ($\alpha_2 = 0.05$). Average lifetimes ($\tau_{AV} = \sum_{i=1}^{2or3}\alpha_i\tau_i$) were 0.75 ps in E13T, 1.10 ps in E13Q, and 0.23 ps in WT, which implies that τ_{AV} was 3.3 times longer in E13T and 4.8 times longer in E13Q, compared to WT. The ultrafast fluorescence dynamics of WT did not change when solvent changed from H_2O to D_2O. Static ET rates (inverse of average lifetimes) were analyzed with static structures of the three systems of FMN-bp. Net electrostatic (ES) energies of Iso and Trp32, on which ET rates depend, were 0.0263 eV in WT, 0.322 eV in E13T, and 0.412 eV in E13Q. The calculated ET rates were in excellent agreement with the observed ones in all systems.

Introduction

Photoinduced electron transfer (ET) in proteins is very important for photosynthetic processes and also for photoreceptors in plants and bacteria.[1] Recently, a number of new flavin photoreceptors have been found.[2−4] In these flavin photoreceptors, cryptochrome and BLUF contain aromatic amino acids as Trp and Tyr near isoalloxazine (Iso). ET from Tyr21 to Iso* in BLUF (blue-light sensing using flavins) of AppA is considered to be a first step of its function.[5−7]

The ultrafast fluorescence dynamics of various "nonfluorescent" flavoproteins were investigated by means of an up-conversion method.[8−10] In these nonfluorescent flavoproteins, Trp and/or Tyr always exist near Iso. Femtosecond transient absorption spectra of these flavoprotein systems revealed that the back ET reaction from the excited to the ground state takes place within 8 ps in riboflavin binding protein and 30 ps in glucose oxidase, after ET from Trp and/or Tyr to the excited flavin.[11]

Three-dimensional structures of WT FMN-bp were determined by X-ray crystallography[12] and NMR spectroscopy.[13] According to these structures, Trp32 was closest to Iso, followed by Tyr-35 and Trp106.

Various ET theories have been modeled for bulk solution.[14−19] It is not yet clear which factor is the most important for ET in proteins. There should be something different between ET processes in protein and ones in bulk solution. The ET rate of FMN-bp was much slower in crystal than in solution,[20] which could not be explained solely by donor−acceptor distance. The results suggest an influential factor for ET in FMN-bp other than donor−acceptor distance, but the reason for it is not yet known. The fluorescence lifetimes were compared among WT, W32Y (Trp-32 was replaced by Tyr-32), and W32A (Trp-32 was replaced by Ala-32) FMN-bps.[21]

Fluorescence dynamics of WT, W32Y, and W32A were simultaneously analyzed with KM theory and atomic coordinates obtained by MD.[22,23] In these works it was found that electrostatic interaction between the Iso anion and other ionic amino acids and between ET donor cations and other ionic amino acids are important. In the present work, we have determined crystal structures of E13T and E13Q where Glu13 with a negative

* Corresponding authors.
† Institute for Laser Technology.
‡ Osaka City University.
§ Mahidol University.

10.1021/jp912137s
Published on Web 04/16/2010

TABLE 1: Crystallographic Data for FMN-bp Mutants

	E13Q	E13T
data collection		
space group	$P2_1$	$P2_1$
unit cell dimensions (Å)	$a = 36.7$, $b = 83.6$, $c = 79.6$, $\beta = 94.7$	$a = 36.9$, $b = 84.9$, $c = 40.2$, $\beta = 91.2$
wavelength (Å)	1.0000	
resolution (Å)	19.68−1.20 (1.27−1.20)	20−1.40 (1.48−1.40)
R_{merge}[a]	0.051 (0.131)	0.058 (0.167)
completeness (%)	94.4 (92.1)	99.7 (99.5)
observed reflections	941773	353799
unique reflections	140127	48510
multiplicity	6.7 (6.5)	7.3 (7.3)
$I/s(I)$	8.2 (5.0)	8.8 (4.2)
refinement		
resolution (Å)	10−1.20	10−1.40
no. of reflections	132890	45935
R factor[b]	0.171	0.156
free R factor	0.190	0.182
rms deviation bond length (Å)	0.011	0.013
rms deviation bond angle (°)	1.425	1.488
no. of water molecules	896	396

[a] $R_{merge} = (\sum_{hkl}|I - \langle I\rangle|)/(\sum_{hkl}\langle I\rangle)$. [b] R factor $= (\sum||F_{obs}| - |F_{calc}||)/(\sum|F_{obs}|)$.

charge was replaced by neutral Thr13 and Gln13, respectively, by the X-ray diffraction method and the ultrafast fluorescence decays of these FMN-bps were compared with one of WT. Accordingly, we can expect the effects of disappearance of one negative charge on ultrafast fluorescence dynamics induced by ET from Trp and/or Tyr to Iso*.

Materials and Methods

Materials and Crystallization. E13T and E13Q (accession number D21804) were prepared basically according to methods described elsewhere.[24] The protein solutions of two mutants were concentrated to 30 mg mL^{-1} in 0.1 M Tris-HCl (pH 7.5). Both mutants were crystallized under conditions similar to those for wild-type FMN-bp.[25] The well-diffracted crystals were grown by vapor diffusion using the hanging-drop method at 4 °C against a reservoir containing 0.1 M Tris-HCl (pH 7.5), 24% (w/v) polyethylene glycol 6000, 0.2 M sodium acetate, and 10% glycerol.

Data Collection and Structural Determination of the FMN-bp Mutants. For the E13Q mutant, diffraction data were obtained at the Photon Factory (Tsukuba, Japan) beamline BL-5A, using an ADSC Quantum 315 CCD detector. For the E13T mutant, diffraction data were obtained at the Photon Factory beamline BL-17A, using an ADSC Quantum 270 CCD detector. Collected data were processed using the programs HKL2000 and SCALA of the CCP4 program suite.[26] The structures of mutants were determined by a molecular replacement (MR) method with the program MOLREP[27] in the CCP4 suite. The search model for MR was derived from the structure of wild-type FMN-bp (Protein Data Bank code 1flm). The resulting models from MR were first refined by rigid body refinement and simulated annealing using the program CNS.[28] Further refinements of the structures of the mutants were carried out using the programs COOT[29] and REFMAC.[30] The atomic coordinates and structural factors for FMN-bp mutants have been deposited in the Protein Data Bank (ID codes 3A6R and 3A6Q for E13Q and E13T, respectively). The crystallographic and refinement data are summarized in Table 1.

Dissociation Constants. The apoFMN-bp was prepared by removing the FMN from the holoprotein under conditions similar to those described previously.[31] The apoFMN-bp was precipitated in 3% trichloroacetic acid (TCA), and then the pellet was washed several times with 3% TCA until both the pellet and the supernatant were not yellow-colored. The pellet, dissolved in 0.1 M sodium phosphate (pH 7.0), was dialyzed against the buffer used for the following analysis. The equilibrium dissociation constants (K_d) of the complexes between FMN and apoFMN-bp mutants were determined by titration of FMN with apoFMN-bp at 25 °C in the dark. In brief, 3 mL of 0.1 μM FMN in 0.05 M sodium phosphate (pH 7.0) containing 0.2 M NaCl was titrated with aliquots of 5−10 μM apoFMN-bp in the same buffer. Complex formation between FMN and apoFMN-bp was monitored by measuring the quenching of FMN fluorescence upon binding to the apoFMN-bp using a spectrofluorometer (F-7000; Hitachi Ltd., Tokyo, Japan) with an excitation wavelength of 445 nm and an emission wavelength of 525 nm. The K_d values were calculated from the titration curves as described previously.[32]

Residue Root of Mean Square Distance between WT and E13T or E13Q. The residue root of mean squre distance (rmsd) between WT and E13T or E13Q was calculated according to the following procedure: (1) The mean coordinates over all atoms of Iso in A and B subunits of WT were obtained. (2) The mean coordinates of Iso in A and B subunits of E13T and in A, B, C, and D subunits of E13Q were also calculated. (3) The coordinates of all atoms in E13T and E13Q were converted into those of the WT coordination system using the mean coordinates of Iso, because Iso is considered to bind firmly with the protein parts. (4) rmsd of a residue i was calculated by eq 1.

$$\mathrm{rmsd}(i) = \frac{1}{n_i}\sum_{j=1}^{n_i}\sqrt{\{X_i^{M}(j) - X_i^{WT}(j)\}^2 + \{Y_i^{M}(j) - Y_i^{WT}(j)\}^2 + \{Z_i^{M}(j) - Z_i^{WT}(j)\}^2} \quad (1)$$

Here, n_i is the number of atoms in the residue i. $X_i^{M}(j)$, $Y_i^{M}(j)$, and $Z_i^{M}(j)$ are x, y, and z coordinates of atom j in a residue i of E13T or E13Q expressed in the coordinate system of WT. $X_i^{WT}(j)$, $Y_i^{WT}(j)$, and $Z_i^{WT}(j)$ are the coordinates of WT.

Measurements of Ultrafast Fluorescence Dynamics. The femtosecond time-resolved fluorescence decays of E13T and E13Q in 10 mM Tris-HCl at pH 8.0 containing 200 mM NaCl were measured using a homemade up-conversion apparatus. A

Ti:Sapphire laser system (Verdi-V8 pumped Mira 900, Coherent, Inc.) was used as a light source (120 fs, 76 MHz, 800 mW at 820 nm). The pulses were further compressed up to ~70 fs fwhm using a prism pair compressor. The second harmonic (~20 mW) was generated in a 0.1 mm thin BBO crystal and focused onto the sample circulating in a flow cell (50 mL/min) with 1 mm light path length, to generate the fluorescence. It was collected with a pair of parabolic mirrors and focused, together with the residual fundamental laser pulse, on a 0.4 mm BBO type I crystal to generate the up-converted signal at the sum frequency. After passing through a grating monochromator (1200 g/mm, Acton Research Corp.), the fluorescence was detected by a photomultiplier (R1527P) coupled with a photon counter (C5410) system (both from Hamamatsu Photonics K. K.). The fluorescence decay curves were obtained by varying the optical path length of the delay stage for the fundamental laser pulse. Ten scans (with 20 fs steps) in alternate directions were accumulated to obtain a single transient with acceptable signal-to-noise ratio. As an instrumental response function, the cross-correlation signal between the fundamental and secondary harmonic pulses was used (fwhm ~130 fs). All measurements were carried out at room temperature (~20 °C). In these experiments, the optical density per 1 cm path length was ~3 at 410 nm.

Calculation of Static ET Rate. The static ET rate was calculated by eq 2, according to Kakitani and Mataga[18,19] (KM theory).

$$k_{\mathrm{ET}}^{ij} = \frac{\nu_0^i}{1 + \exp\{\beta^i(R_j^i - R_0^i)\}}\sqrt{\frac{k_{\mathrm{B}}T}{4\pi\lambda_{\mathrm{S}}^{ij}}} \times \exp\left[-\frac{\{\Delta G_i^0 - e^2/\varepsilon_0^j R_j^i + \lambda_{\mathrm{S}}^{ij} + \mathrm{ES}_j^i\}^2}{4\lambda_{\mathrm{S}}^{ij}k_{\mathrm{B}}T}\right] \quad (2)$$

Here i and j denote Trp or Tyr, and one of the three FMN-bp proteins, WT, E13T, and E13Q, respectively. Here, $\nu_0{}^i$ is an adiabatic frequency, and β^i is an ET process coefficient. R_j^i and $R_0{}^i$ are the donor−acceptor distance between Iso and Trp or Tyr in the protein j and a critical donor−acceptor distance for the ET process, respectively. R_j^i was expressed as a center-to-center distance rather than an edge-to-edge distance.[22,23] The ET process is adiabatic when $R_j^i < R_0{}^i$ and nonadiabatic when $R_j^i > R_0{}^i$. k_{B}, T, and e are Boltzmann constant, temperature, and electron charge, respectively. ES_j^i is an electrostatic energy between the ET acceptor anion + donor cation (i) and all other ionic groups in the proteins in the protein j,[22,23] as described bellow.

$\lambda_{\mathrm{S}}{}^{ij}$ is known as solvent reorganization energy[14,15] of ET donor i in the protein j and expressed as eq 3.

$$\lambda_{\mathrm{S}}^{ij} = e^2\left(\frac{1}{2a_1} + \frac{1}{2a_2} - \frac{1}{R_j^i}\right)\left(\frac{1}{\varepsilon_\infty} - \frac{1}{\varepsilon_0^j}\right) \quad (3)$$

where a_1 and a_2 are radii of the acceptor and donor when these reactants are assumed to be spherical, and ε_∞ and $\varepsilon_0{}^j$ are optical constant and static dielectric constant of the protein j. The optical dielectric constant used was 2.0. The value of a_1 of Iso was 0.224 nm, and that of a_2 for Trp and Tyr was 0.196 and 0.173 nm, respectively.[22,23]

The standard free energy change was expressed with ionization potential of ET donor, E_{IP}, as eq 4.

$$\Delta G_i^0 = E_{\mathrm{IP}}^i - G_{\mathrm{Iso}}^0 \quad (4)$$

$G_{\mathrm{Iso}}{}^0$ is standard Gibbs energy related to electron affinity of Iso*. The values of $E_{\mathrm{IP}}{}^i$ were 7.2 eV for Trp and 8.0 eV for Tyr, respectively.[33]

Protein systems contain many ionic groups, which may influence ET rate. ES energy between Iso^- and all ionic groups including phosphate anions of FMN in the FMN-bp system j [ES_j(Iso)], between $\mathrm{Trp32}^+$ and all ionic groups in the FMN-bp system j [ES_j(Trp32)], between $\mathrm{Tyr35}^+$ and all ionic groups in the FMn-bp system j [ES_j(Tyr35)], and between $\mathrm{Trp106}^+$ and all ionic groups in FMN-bp system j [ES_j(Trp106)] are expressed by eqs 5−8, respectively. WT FMN-bp contains 8 Glu's, 5 Asp's, 4 Lys's, 9 Arg's, and 2 negative charges at FMN phosphate. The number of Glu is denoted as n in eqs 5−8. The values of n are 8 in WT and 7 in both E13T and E13Q.

$$\mathrm{ES}_j(\mathrm{Iso}) = \sum_{i=1}^{n}\frac{C_{\mathrm{Iso}}\cdot C_{\mathrm{Glu}}}{\varepsilon_0^j R_j^{\mathrm{Iso}}(\mathrm{Glu}-i)} + \sum_{i=1}^{5}\frac{C_{\mathrm{Iso}}\cdot C_{\mathrm{Asp}}}{\varepsilon_0^j R_j^{\mathrm{Iso}}(\mathrm{Asp}-i)} + \sum_{i=1}^{4}\frac{C_{\mathrm{Iso}}\cdot C_{\mathrm{Lys}}}{\varepsilon_0^j R_j^{\mathrm{Iso}}(\mathrm{Lys}-i)} + \sum_{i=1}^{9}\frac{C_{\mathrm{Iso}}\cdot C_{\mathrm{Arg}}}{\varepsilon_0^j R_j^{\mathrm{Iso}}(\mathrm{Arg}-i)} + \sum_{i=1}^{2}\frac{C_{\mathrm{Iso}}\cdot C_{\mathrm{P}}}{\varepsilon_0^j R_j^{\mathrm{Iso}}(\mathrm{P}-i)} \quad (5)$$

$$\mathrm{ES}_j(\mathrm{Trp32}) = \sum_{i=1}^{n}\frac{C_{32}\cdot C_{\mathrm{Glu}}}{\varepsilon_0^j R_j^{32}(\mathrm{Glu}-i)} + \sum_{i=1}^{5}\frac{C_{32}\cdot C_{\mathrm{Asp}}}{\varepsilon_0^j R_j^{32}(\mathrm{Asp}-i)} + \sum_{i=1}^{4}\frac{C_{32}\cdot C_{\mathrm{Lys}}}{\varepsilon_0^j R_j^{32}(\mathrm{Lys}-i)} + \sum_{i=1}^{9}\frac{C_{32}\cdot C_{\mathrm{Arg}}}{\varepsilon_0^j R_j^{32}(\mathrm{Arg}-i)} + \sum_{i=1}^{2}\frac{C_{32}\cdot C_{\mathrm{P}}}{\varepsilon_0^j R_j^{32}(\mathrm{P}-i)} \quad (6)$$

$$\mathrm{ES}_j(\mathrm{Tyr35}) = \sum_{i=1}^{n}\frac{C_{35}\cdot C_{\mathrm{Glu}}}{\varepsilon_0^j R_j^{35}(\mathrm{Glu}-i)} + \sum_{i=1}^{5}\frac{C_{35}\cdot C_{\mathrm{Asp}}}{\varepsilon_0^j R_j^{35}(\mathrm{Asp}-i)} + \sum_{i=1}^{4}\frac{C_{35}\cdot C_{\mathrm{Lys}}}{\varepsilon_0^j R_j^{35}(\mathrm{Lys}-i)} + \sum_{i=1}^{9}\frac{C_{35}\cdot C_{\mathrm{Arg}}}{\varepsilon_0^j R_j^{35}(\mathrm{Arg}-i)} + \sum_{i=1}^{2}\frac{C_{35}\cdot C_{\mathrm{P}}}{\varepsilon_0^j R_j^{35}(\mathrm{P}-i)} \quad (7)$$

$$\mathrm{ES}_j(\mathrm{Trp106}) = \sum_{i=1}^{n}\frac{C_{106}\cdot C_{\mathrm{Glu}}}{\varepsilon_0^j R_j^{106}(\mathrm{Glu}-i)} + \sum_{i=1}^{5}\frac{C_{106}\cdot C_{\mathrm{Asp}}}{\varepsilon_0^j R_j^{106}(\mathrm{Asp}-i)} + \sum_{i=1}^{4}\frac{C_{106}\cdot C_{\mathrm{Lys}}}{\varepsilon_0^j R_j^{106}(\mathrm{Lys}-i)} + \sum_{i=1}^{9}\frac{C_{106}\cdot C_{\mathrm{Arg}}}{\varepsilon_0^j R_j^{106}(\mathrm{Arg}-i)} + \sum_{i=1}^{2}\frac{C_{106}\cdot C_{\mathrm{P}}}{\varepsilon_0^j R_j^{106}(\mathrm{P}-i)} \quad (8)$$

In eqs 5−8, C_{Iso} is the charge of the Iso anion and is equal to $-e$. C_{32}, C_{35}, and C_{106} are charges of the Trp32 cation, Tyr35 cation, and Trp106 cation, respectively, and all are equal to $+e$. C_{Glu} and C_{Asp} are the charges of Glu and Asp, respectively, and equal to $-e$. C_{Lys} and C_{Arg} are the charges of Lys and Arg, respectively, and equal to $+e$. C_{P} is the charge of phosphate of

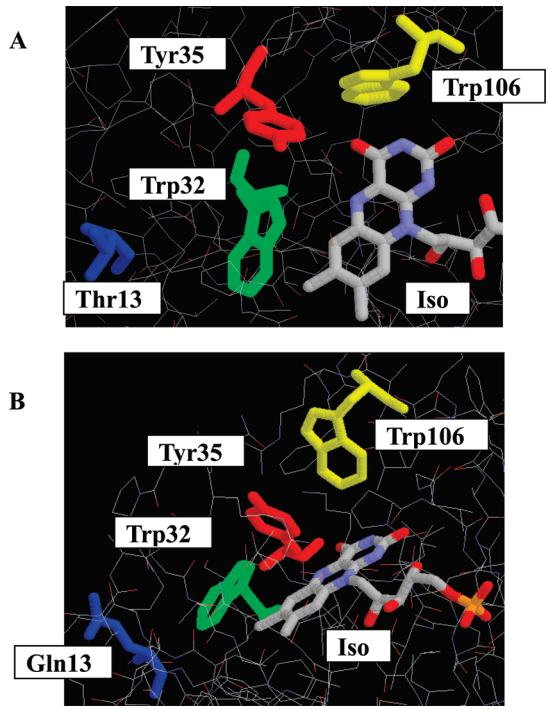

Figure 1. X-ray structures of E13T and E13Q near Iso binding site A, E13T, and B, E13Q.

FMN and is equal to $-e$. We assumed that these groups were all in an ionic state in solution. Distances between Iso and the ith Glu ($i = 1 - n$) in the FMN-bp system j are denoted as $R_j^{\mathrm{Iso}}(\mathrm{Glu} - i)$. Distances between Trp32 and the ith Glu ($i = 1 - n$) are denoted as $R_j^{32}(\mathrm{Lys} - i)$, and so on. Here, ES energies were evaluated with using only ionic groups in the proteins. When ES energies were obtained with all partial charge densities in the protein, they did not differ much from those of the present method (unpublished work).

ES_j^i in eq 2 was expressed as follows

$$\text{For } k_j^{\mathrm{Trp32}},\ \mathrm{ES}_j^{\mathrm{Trp32}} = \mathrm{ES}_j(\mathrm{Iso}) + \mathrm{ES}_j(\mathrm{Trp32}) \quad (9)$$

$$\text{For } k_j^{\mathrm{Tyr35}},\ \mathrm{ES}_j^{\mathrm{Tyr35}} = \mathrm{ES}_j(\mathrm{Iso}) + \mathrm{ES}_j(\mathrm{Tyr35}) \quad (10)$$

$$\text{For } k_j^{\mathrm{Trp106}},\mathrm{ES}_j^{\mathrm{Trp106}} = \mathrm{ES}_j(\mathrm{Iso}) + \mathrm{ES}_j(\mathrm{Trp106}) \quad (11)$$

k_j^{Trp32}, k_j^{Tyr35}, and k_j^{Trp106} denote ET rates from Trp32, Tyr106, and Trp106 to Iso* in the FMN-bp system j, respectively.

The values of ES energy given by eqs 5−8 and, consequently, ES_j^i given by eqs 9−11 were separately evaluated among WT, E13T, and E13Q because distances between the Iso anion and ionic groups and between the cations and ionic groups were different among these systems.

ET parameters contained in eq 2 were determined to obtain the calculated average lifetimes to be equal to the observed ones. ES energies and ET rates were calculated by the two methods. The ET parameters were determined in the present work in Method A, and the reported ET parameters[23] were used to calculate ET rates in Method B. The donor−acceptor distances were evaluated by X-ray structures of WT, E13T, and E13Q.

Results

Structures of E13T and E13Q in Crystal. Figure 1 shows X-ray structures of E13T in A and E13Q in B near the FMN binding site. In addition to Iso, Trp32, Tyr35, and Trp106, Thr13 in A and Gln13 in B were also illustrated by a stick model. Geometrical factors near FMN binding sites were compared among X-ray structures of WT, E13T, and E13Q as shown by Table 2. Center-to-center distances between the amino acid at 13 and Iso, R(IsoRes13), were 1.06 nm in WT, 1.48 nm in E13T, and 1.39 nm in E13Q. The distances between the amino acid at

TABLE 2: Comparison of FMN-bp Structures at the Iso Binding Site[a]

geometrical factor	WT[b] (X-ray)	E13T[c] (X-ray)	E13Q[d] (X-ray)	WT[e] (NMR)	WT[f] (MD)
R(IsoRes13)[g]	1.06	1.48	1.39	1.33	1.50
R(32Res13)[g]	0.510	0.873	0.767	0.620	0.991
R(35Res13)[g]	0.674	1.210	1.043	0.904	0.956
R(106Res13)[g]	1.27	1.78	1.60	1.47	1.50
R(Iso32)[h]	0.705	0.712	0.708	0.842	0.642
R(Iso35)[h]	0.772	0.761	0.765	0.736	1.05
R(Iso106)[h]	0.851	0.837	0.839	0.815	0.988
Angle (Iso32)[i]	–47.6	–50.4	–50.6	–19.7	12.2
Angle (Iso35)[i]	–69.0	69.8	71.4	–65.6	79.3
Angle (Iso106)[i]	79.6	77.9	78.5	75.2	82.6

[a] Distance was expressed in units of nanometers. [b] Data reported by Suto et al.[24] [c] Glu13 was replaced by Thr13. [d] Glu13 was replaced by Gln13. [e] Data reported by Liepinsh et al.[25] Mean values of 20 structures were listed. [f] Data reported by Nunthaboot et al.[23] [g] R(IsoRes13) denotes distance between Iso and Glu13 in WT (Thr13 in E13T, Gln13 in E13Q). R(32Res13) denotes distance between Trp32 and Glu13 in WT (Thr13 in E13T, Gln13 in E13Q), and so on. The position of Glu13 was expressed by coordinates of the center of two O atoms of the side chain. The position of Thr13 was expressed by coordinates of the O atom of the side chain. The position of Gln13 was expressed by coordinates of the center between N and O atoms of the side chain. [h] R(Iso32), R(Iso35), and R(Iso106) represent center to center distances between Iso and Trp32, between Iso and Tyr35, and between Iso and Trp106, respectively. [i] Interplanar angles between Iso and aromatic amino acid residues of Trp32, Tyr35, and Trp106.

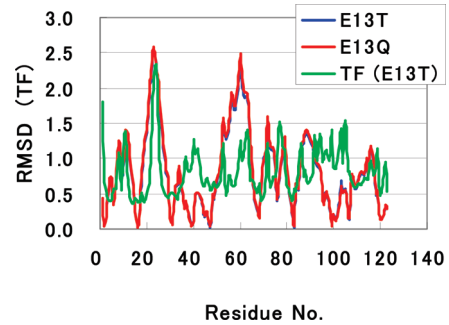

Figure 2. rmsd between WT and E13T or E13Q. E13T and E13Q indicate residue rmsd's between WT and E13T and between WT and E13Q. rmsd is represented in units of nanometers. TF (E13T) denotes the residue temperature factor of E13T.

TABLE 3: Amino Acid Residues with Low and High Residue rmsd

E13T and E13Q FMN-bp	
low residue rmsd	high residue rmsd
Met1-Leu2-Pro3	Lys11-Asn12-Glu13
Val15-Val16-Ala17	Gln21-Gly22-Glu23
Asn30-Thr31-Trp32	Val58-Ala59-Arg60
Leu39-Asp40-Gly41	Arg71-Lys72-Val73
Val46-Pro47-Val48	Gly78-Pro79-Gly80
Thr67-Leu68-Gly69	Ser88-Ala89-Ala90
Gly82-Phe83-Leu84	Ile113-Thr114-Val115
Phe98-Glu99-Ala100	
Trp106-Ala107-Arg108	
Gln120-Thr121-Lue122	

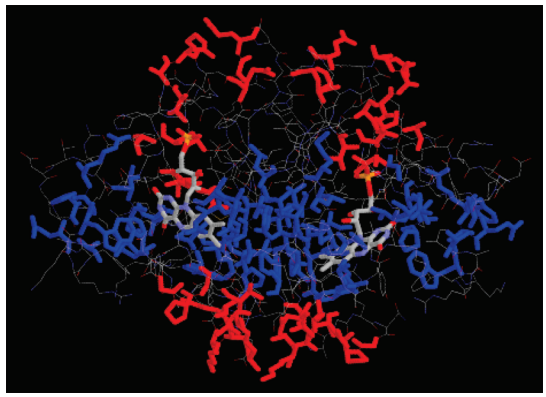

Figure 3. Structural similarity of E13T with WT FMN-bp in crystal. Amino acid residues with relatively high rmsd are shown in red and those with relatively low rmsd in blue. The interface between the two subunits exists at a center vertical line. The structure of E13T was quite different from WT at the top and bottom parts and quite similar with WT at the middle part.

13 and Trp32 were 0.51 nm in WT, 0.873 nm in E13T, and 0.767 nm in E13Q. The distances between the amino acid at 13 and Tyr35 were 0.674 nm in WT, 1.21 nm in E13T, and 1.60 nm in E13Q. Great differences in the distances among the three forms of FMN-bp may be ascribed to different lengths of chains of amino acid residues at 13. The distances between Iso and nearby aromatic amino acid residues did not change appreciably among the three forms. The distances were 0.705 nm in WT, 0.712 nm in E13T, and 0.708 nm in E13Q. Interplanar angles between Iso and Tyr35 remarkably changed among the three forms, though the angles between Iso and Trp32 or Trp106 were not different appreciably. The angles between Iso and Tyr35 were −69° in WT, 70° in E13T, and 71° in E13Q. These geometrical factors obtained by NMR spectroscopy and molecular dynamic simulation are also listed in Table 2 for comparison.

Structural Similarity between WT and the Mutated FMN-bp. Figure 2 shows the residue root of mean square distance (rmsd) between WT and E13T or E13Q. The values of rmsd in E13T were almost identical with those in E13Q. The crystal structure of E13T or E13Q was quite different from WT at amino acids around 12 (Asn), 22 (Gly), 59 (Ala), 72 (Lys), 79 (Pro), and 114 (Thr), while it was similar with WT at around 2 (Leu), 16 (Val), 31 (Thr), 40 (Asp), 47 (Pro), 68 (Leu), 83 (Phe), 99 (Glu), 107 (Ala), and 121 (Thr). Table 3 lists amino acid residues with low and high rmsd. Figure 3 shows structural similarity between WT and E13T. Amino acid residues in blue displayed the amino acids with relatively low rmsd, which implies that local structures of E13T around these amino acids are quite similar with those of WT. On the other hand, the local structures at amino acid residues in red (with relatively high rmsd) are considered to be quite different from those of WT. The structure of E13T was similar with WT at the middle part but quite different from WT at the top and bottom parts.

TABLE 5: Dissociation Constant of FMN and Concentration of Free FMN[a]

FMN-bp	K_d (nM)	[FMN] (nM)[b]	[FMN]/[Protein] (%)[b]
WT[c]	0.465	30–37	0.12–0.15
E13T	1.39 ± 0.25	53–65	0.22–0.26
E13Q	0.90 ± 0.10	42–52	0.17–0.21

[a] Each value is the average of at least three independent measurements. [b] Calculated with K_d and the concentrations of the proteins at the fluorescence measurements (0.2−0.3 mM). [c] Kitamura et al.[32]

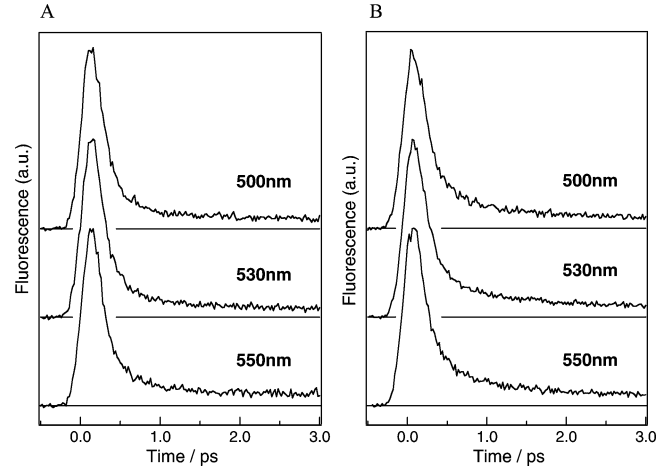

Figure 4. Fluorescence decay curves monitored at different wavelengths. A: E13T. B: E13Q. Both were excited at 410 nm. No wavelength dependence of the decays was observed in either E13T or E13Q.

TABLE 4: Hydrogen Bondings between Iso and Nearby Amino Acids[a]

FMN-bp	subunit	Iso/amino acid	distance (nm)	FMN-bp	subunit	Iso/amino acid	distance (nm)
WT	A	O2/Gly49 NH[b]	0.279	E13Q	A	O2/Gly49NH[b]	0.278
		N3H/Pro47O[c]	0.298			O2/Gly50NH[b]	0.297
		O4/Thr31OH	0.277			N3H/Pro47O[c]	0.297
						O4/Thr31OH	0.275
	B	O2/Gly49 NH	0.282		B	O2/Gly49NH	0.275
		O2/Gly50NH	0.297			O2/Gly50NH	0.294
		N3H/Pro47O	0.295			N3H/Pro47O	0.293
		O4/Thr31OH	0.278			O4/Thr31OH	0.277
E13T	A	O2/Gly49 NH	0.277		C	O2/Gly49NH	0.277
		O2/Gly50NH	0.298			O2/Gly50NH	0.296
		N3H/Pro47O	0.299			N3H/Pro47O	0.295
		O4/Thr31OH	0.270			O4/Thr31OH	0.276
	B	O2/Gly49 NH	0.277		D	O2/Gly49NH	0.277
		O2/Gly50NH	0.294			O2/Gly50NH	0.296
		O4/Thr31OH	0.273			N3H/Pro47O	0.292
						O4/Thr31OH	0.279

[a] The proton donor/acceptor pairs with the distance shorter than 0.3 nm were collected. The mean distances were 0.278 ± 0.0008 nm in O2/Gly49NH, 0.297 ± 0.0010 nm in O2/Gly50NH, 0.297 ± 0.0012 nm in N3H/Pro47O, and 0.276 ± 0.0011 nm in O4/Thr31OH. [b] Peptide NH. [c] Peptide O.

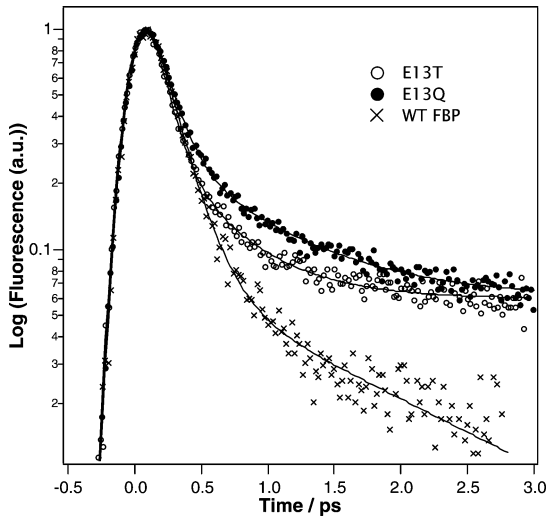

Figure 5. Ultrafast fluorescence dynamics of E13Q, E13T, and WT. Fluorescence intensities are indicated by open circles for E13T, closed circles for E13Q, and x marks for WT,[20,21] which is shown for comparison. Emissions were monitored at 530 nm for all FMN-bps. Solid lines show the calculated decay curves with the best-fit decay parameters with multiexponential functions. Fluorescence lifetimes of E13T were 107 fs (86%), 475 fs (12%), and 30 ps (2%). The lifetimes of E13Q were 134 fs (85%), 746 fs (12%), and 30 ps (3%). The lifetimes of WT[20,21] were 168 fs (95%) and 1.4 ps (5%).

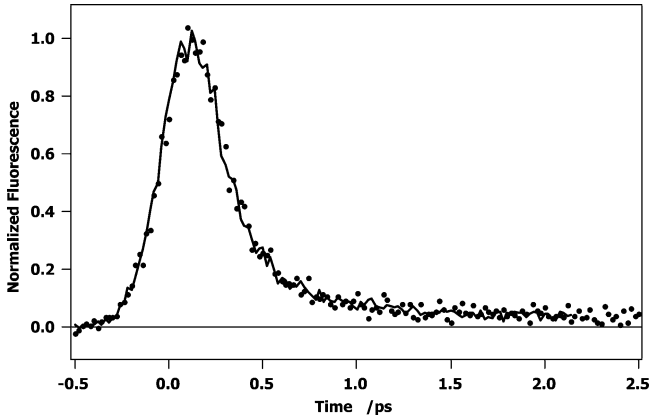

Figure 6. Comparison of fluorescence decay dynamics of WT in H_2O (solid line) and in D_2O (filled circles) monitored at 530 nm.

Comparison of Temperature Factors among the Three Forms of FMN-bp. The temperature factor of each residue was evaluated by taking the average of the temperature factors of constituent atoms in a residue. Temperature factors were much higher in WT than those in E13T and E13Q. This may be ascribed to the nature of crystals. However, amino acid residues with peak temperature factor were common among the three proteins. Amino acids with the peak were Glu8, Lys11, Glu23, Asp49, Lys53, Arg60, Glu62, Lys72, Asn77, Arg86, Arg92, Arg103, and Glu119. Residue temperature factors of E13T were shown in Figure 2. These amino acids mostly contain charges with aliphatic chains. Some of the amino acids with peak temperature factors coincided with those with high rmsd.

Hydrogen Bonds in Iso. O2 of Iso in WT forms hydrogen bondings with peptide NHs of Gly49 and Gly50, N3H with peptide O of Pro47, and O4 with Thr31OH. These hydrogen bonding pairs did not alter in E13T and E13Q. Table 4 compares the bond distances among three proteins. The hydrogen bond distances were also not modified appreciably in the mutated FMN-bps. The mean distances taken over all proteins and subunits were 0.278 ± 0.0008 nm in O2/Gly49NH, 0.297 ± 0.0010 nm in O2/Gly50NH, 0.297 ± 0.0012 nm in N3H/Pro47O, and 0.276 ± 0.0011 nm in O4/Thr31OH.

Dissociation Constants of FMN. Dissociation constants (K_d) of FMN in E13T and E13Q were determined and listed in Table 5. The values of K_d were 1.39 ± 0.25 nM in E13T and 0.90 ± 0.10 nM in E13Q. The concentrations of free FMN dissociated from the proteins and ratios of the concentration of free FMN to one of the proteins are also listed in Table 5. The values of K_d were not very different with one of WT[32] (0.465 nM). The concentration ratios were 0.12–0.15% in WT, 0.22–0.26% in E13T, and 0.17–0.21% in E13Q.

Ultrafast Fluorescence Dynamics of E13T and E13Q. The fluorescence decays in the femtosecond−picosecond time domain are shown in Figure 4. The decays of both E13T and E13Q did not change appreciably when the emission monitored changed from 500 to 550 nm. The fluorescence decays were compared among E13T, E13Q, and WT as in Figure 5. The fluorescence decay of WT was obtained in the previous work.[20,21] The decay parameters of E13T were $\tau_1 = 107$ fs ($\alpha_1 = 0.86$), $\tau_2 = 475$ fs ($\alpha_2 = 0.12$), and $\tau_3 = 30$ ps ($\alpha_3 = 0.02$). The decay parameters of E13Q were $\tau_1 = 134$ fs ($\alpha_1 = 0.85$), $\tau_2 = 746$ fs ($\alpha_2 = 0.12$), and $\tau_3 = 30$ ps ($\alpha_3 = 0.03$).

TABLE 6: ES Energy and ET Rate[a]

protein system	method	ES energy[b] (eV)				net ES energy[c](eV)			ES energy between the Iso anion and the donor cation[d] (eV)			calculated ET rate[e] (ps^{-1})			τ_{calc}[f] (ps)	τ_{obs} (ps)
		Iso	Trp32	Tyr35	Trp106	Trp32	Tyr35	Trp106	Trp32	Tyr35	Trp106	Trp32	Tyr35	Trp106		
WT	A[g]	0.173	–0.147	0.0159	0.0191	0.0263	0.189	0.193	–0.254	–0.232	–0.211	3.71	0.0423	0.599	0.230[g]	0.230
	B[h]	0.141	–0.120	0.0130	0.0156	0.0214	0.154	0.157	–0.207	–0.189	–0.172	1.82	8.24×10^{-5}	0.0589	0.533[h]	0.230
E13T	A[g]	–0.0371	0.359	0.484	0.273	0.322	0.447	0.236	–0.390	–0.364	–0.332	0.981	0.188	0.164	0.750[g]	0.750
	B[h]	–0.0195	0.189	0.255	0.144	0.169	0.235	0.124	–0.205	–0.192	–0.174	1.45	3.99×10^{-5}	0.0888	0.651[h]	0.750
E13Q	A[g]	0.0177	0.394	0.496	0.297	0.412	0.514	0.315	–0.435	–0.403	–0.367	0.530	0.290	0.0891	1.10[g]	1.10
	B[h]	0.0084	0.187	0.235	0.141	0.195	0.244	0.149	–0.206	–0.191	–0.174	1.52	3.44×10^{-5}	0.0798	0.623[h]	1.10

[a] The ES energies and ET rates were obtained by the two methods, A and B, and expressed as the mean of two subunits in WT and E13T and four subunits in E13Q. [b] Electrostatic energies between ET donors or acceptor and all other ionic groups in the proteins, given by eqs 5−8. [c] Net ES energies were calculated by eqs 9−11. [d] ES energy between the Iso anion and cation of an ET donor was obtained by equations, $-e^2/\varepsilon_0^i R_j^i$ (see eq 2), where i is Trp or Tyr and j is one of WT, E13T, or E13Q. [e] ET donors are indicated. ET rates were calculated by two methods, one with ET parameters taken from the previous work[23] (see also footnote g) and another with ET parameters determined in the present work shown in footnote a. [f] τ_{calc} was calculated by an equation, 1/{Rate(32) + Rate(35) + Rate(106)}, where Rate(32), Rate(35), and Rate(106) are ET rates from Trp32, Try35, and Trp106 to the excited Iso, respectively. [g] ET parameters were determined in the present work, to obtain the calculated average lifetimes equal to the observed ones. $\nu_0^{Trp} = 1016$ (ps^{-1}), $\nu_0^{Tyr} = 197$ (ps^{-1}), $\beta_{Trp} = 21.0$ (nm^{-1}), $\beta_{Tyr} = 6.25$ (nm^{-1}), $R_0^{Trp} = 0.663$ (nm), $R_0^{Tyr} = 0.499$ (nm), $G_{Iso} = 9.22$ (eV). The values of ε_0 were 8.03 in WT, 5.19 in E13T, and 4.67 in E13Q. ET rates and τ_{calc} were calculated with these ET parameters. [h] The ET rates were calculated with ET parameters reported in the previous work.[23] ET parameters[23] were $\nu_0^{Trp} = 1016$ (ps^{-1}), $\nu_0^{Tyr} = 197$ (ps^{-1}), $\beta_{Trp} = 21.0$ (nm^{-1}), $\beta_{Tyr} = 6.25$ (nm^{-1}), $R_0^{Trp} = 0.570$ (nm), $R_0^{Tyr} = 0.0$ (nm), $G_{Iso} = 8.97$ (eV). The values of ε_0 were all 9.86.

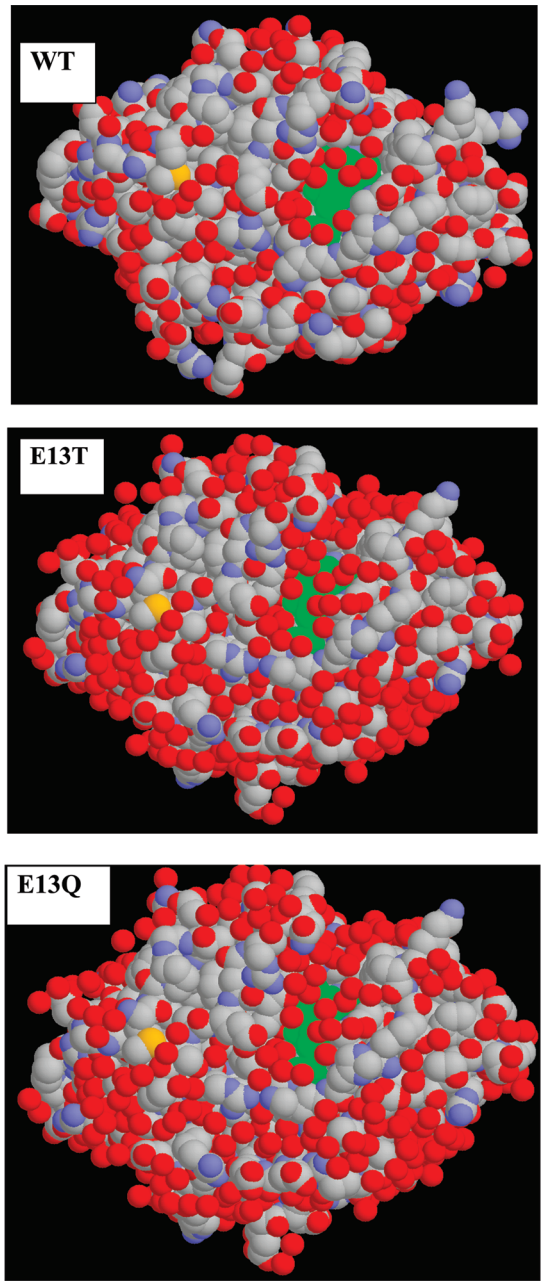

Figure 7. Locations of Iso in the three systems of FMN-bp. Protein structures displayed with the space-filling model. Green balls show Iso atoms.

Fluorescence lifetimes of WT[20] were $\tau_1 = 168$ fs ($\alpha_1 = 0.95$) and $\tau_2 = 1.4$ ps ($\alpha_2 = 0.05$). Average lifetimes ($\tau_{AV} = \sum_{i=1}^{2or3}\alpha_i\tau_i$) were 0.75 ps in E13T, 1.10 ps in E13Q, and 0.23 ps in WT, which implies that τ_{AV} was 3.3 times longer in E13T and 4.8 times longer in E13Q, compared to WT. A remarkable difference in the decays between E13T or E13Q and WT was the appearance of the longest lifetime component (τ_3). The longest lifetime components in both E13T and E13Q were not observed in WT and are considered to be from the bound Iso, not free Iso from the protein moiety, because the concentration ratios between free FMN and the proteins were 1 order of magnitude (0.2−0.3% in Table 5) less than α_3 (2−3%). Another reason why α_3 should not be related to free FMN is that the lifetime of free FMN is 5 ns, of which fluorescence decay should be just flat in the time domain of the present work.

Fluorescence dynamics of WT were measured in deuterium oxide and compared with one in H_2O.[20,21] As we can see from Figure 6, the fluorescence dynamics of WT did not change at all upon the replacement of solvent from H_2O to D_2O.

ES Energies and ET Rates. ES energies given by eqs 5−8 and net ES energies given by eqs 9−11 are listed in Table 6. These energies were calculated with X-ray crystal structures. In Method A these quantities were calculated with ET parameters determined in the present work: $\nu_0^{Trp} = 1016$ (ps^{-1}), $\nu_0^{Tyr} = 197$ (ps^{-1}), $\beta_{Trp} = 21.0$ (nm^{-1}), $\beta_{Tyr} = 6.25$ (nm^{-1}), $R_0^{Trp} = 0.663$ (nm), $R_0^{Tyr} = 0.499$ (nm), $G_{Iso} = 9.22$ (eV). The values of ε_0 were 8.03 in WT, 5.19 in E13T, and 4.67 in E13Q. In Method B the energies and ET rates were calculated with ET parameters reported:[23] $\nu_0^{Trp} = 1016$ (ps^{-1}), $\nu_0^{Tyr} = 197$ (ps^{-1}), $\beta_{Trp} = 21.0$ (nm^{-1}), $\beta_{Tyr} = 6.25$ (nm^{-1}), $R_0^{Trp} = 0.570$ (nm), $R_0^{Tyr} = 0.0$ (nm), $G_{Iso} = 8.97$ (eV). The values of ε_0 were 9.86 in all FMN-bp systems. Here ES energies and ET rates obtained by Method A are described. The values of ES_j(Iso) were 0.173 eV in WT, −0.0371 eV in E13T, and 0.0177 eV in E13Q. The values of ES_j(Trp32) were −0.147 in WT, 0.359 eV in E13T, and 0.394 eV in E13Q. Those of ES_j(Tyr35) were 0.0159 eV in WT, 0.484 eV in E13T, and 0.496 eV in E13Q. Those of ES_j(Trp106) were 0.0191 eV in WT, 0.273 eV in E13T, and 0.297 eV in E13Q. The ET rate depends on a net ES energy given by eqs 9−11. The values of ES_j^{Trp32} were 0.0263 eV in WT, 0.322 eV in E13T, and 0.412 eV in E13Q. Those of ES_j^{Tyr35} were 0.189 eV in WT, 0.447 eV in E13T, and 0.514 eV in E13Q. Those of ES_j^{Trp106} were 0.193 eV in WT, 0.236 eV in E13T, and 0.315 eV in E13Q. ES energies between the donor and acceptor are expressed by $-e^2/\varepsilon_0^i R_j^i$, where i is Trp or Tyr and j is one of WT, E13T, or E13Q. ES energies between the donor cation and acceptor anion in WT were −0.254 eV in Trp32, −0.232 eV in Tyr35, and −0.211 eV in Trp106. The energies in E13T were −0.390 eV in Trp32, −0.364 eV in Tyr35, and −0.332 eV in Trp106. The energies in E13Q were −0.435 eV in Trp32, −0.403 eV in Tyr35, and −0.367 eV in Trp106. ET rates in WT were 3.71 (ps^{-1}) from Trp32, 0.0423 (ps^{-1}) from Tyr35, and 0.599 (ps^{-1}) from Trp106. ET rates in E13T were 0.981 (ps^{-1}) from Trp32, 0.188 (ps^{-1}) from Tyr35, and 0.164 (ps^{-1}) from Trp106. ET rates in E13Q were 0.530 (ps^{-1}) from Trp32, 0.290 (ps^{-1}) from Tyr35, and 0.0891 (ps^{-1}) from Trp106. τ_{calc} calculated by an equation, 1/{Rate(32) + Rate(35) + Rate(106)}, were 0.230 (ps) in WT, 0.750 (ps) in E13T, and 1.10 (ps) in E13Q, which were all in excellent accordance with τ_{obs}. In Method B the agreements between τ_{calc} and τ_{obs} were not very good in all systems.

Discussion

It was reported that fluorescence lifetimes of WT in crystal were much longer than those in solution (20 times in an average lifetime).[20] This could not be explained solely by the donor−acceptor distances. The most drastic change in the environment surrounding the protein in the liquid phase from one in the crystal phase is the presence of water molecules with motional freedom. It is conceivable that fast vibrational−rotational motions of water molecules at relatively distant places from the donors and acceptors in the proteins have an influence on the ET rates. We can expect something different in the fluorescence decays of WT in H_2O buffer and in D_2O buffer solutions because the vibrational motion of O−D in D_2O is slower than that of O−H in H_2O. From Figure 6 it is evident that fluorescence dynamics or the ET rate did not change at all when solvent molecules changed from H_2O to D_2O. This suggests that the vibrational motion of water molecules surrounding the protein does not influence the ET rate, though many motional modes such as rotations and librations other than O−H vibration in liquid water may be influential upon the ET rates.

In the present work, we have demonstrated that the disappearance of only one negative charge of Glu13 substantially influenced the fluorescence dynamics of FMN-bp, or ET rate. ET rates were fastest from Trp32 to Iso* in all systems. Net ES energies of ES_j^{Trp32} given by eq 9, on which ET rates depend, were 0.0263 eV in WT, 0.322 eV in E13T, and 0.496 eV in E13Q. The energy of WT was about 7% of those of E13T and E13Q, which may be responsible for the longer averaged lifetimes of E13T and E13Q, compared to WT. The calculated ET rates or lifetimes in all FMN-bp systems were in excellent agreement with the observed ones. The ET parameters were obtained in the previous work, assuming that ε_0 does not change among three systems of FMN-bp. The assumption may not be valid if the results of analysis of fluorescence dynamics in flavin photoreceptors of AppA[34,35] are considered. In AppA, ε_0 depended on the WT and mutated protein systems, and thereby excellent agreements were obtained between the observed and calculated fluorescence dynamics of all systems. From the present work, we may conclude that (1) electrostatic energy is an influential factor for the ET in proteins, which is different from ET processes in bulk solution, that (2) the reason why the ET rate of FMN-bp in crystal phase is slower than the one in the liquid phase is that the charge state of FMN-bp in crystal[20] may be modified from the one in solution, and (3) that the influence of OH vibrational motion on ET rates is negligible. The slower lifetime of FMN-bp in the crystal phase cannot be ascribed to the absence of librating water molecules. It may be difficult, by X-ray crystallography, to identify the protonation state of ionic amino acids in crystal. Some ionic amino acids in FMN-bp may be protonated without surrounding water molecules. Callis and Liu[36] emphasized the importance of charges for ET in flavin reductase and flavodoxin reductase. Our results are in accordance with their results.

Iso in FMN-bp locates quite close to the water layer as shown in Figure 7. Some of the water molecules may be accessible to the excited Iso. The space between the water layer and Iso is the largest in WT, which may contribute to the greatest ε_0 in WT among the three systems. The disappearance of one charge may also contribute to reduction of ε_0 in E13T and E13Q.

References and Notes

(1) (a) Marcus, R.; Sutin, N. *Biochim. Biophys. Acta* **1985**, *811*, 265. (b) Gray, H. B.; Winkler, J. R. *Annu. Rev. Biochem.* **1996**, *65*, 537. (c) Bendall, D. S. *Protein Electron Transfer*; Kluwer Academic Publishers: New York, 1996.

(2) Grosson, S.; Moffat, K. *Proc. Natl. Acad. Sci. U.S.A.* **2001**, *98*, 2995.

(3) Bouly, J.-P.; Schleicher, E.; Dionisio-Sese, M.; Vandenbussche, F.; van den Straeten, D.; Bakrim, N.; Meier, S.; Batschauer, A.; Galland, P.; Bittl, R.; Ahmad, M. *J. Biol. Chem.* **2007**, *282*, 9383.

(4) Song, S.-H.; Öztürk, N.; Denaro, T. R.; Arat, N. Ö; Kao, Y.-T.; Zhu, H.; Zhong, D.; Reppert, S. M.; Sancar, A. *J. Biol. Chem.* **2007**, *282*, 17608.

(5) Anderson, S.; Dragnea, V.; Masuda, S.; Ybe, J.; Moffat, K.; Bauer, C. *Biochemistry* **2005**, *44*, 7998.

(6) Yuan, H.; Anderson, S.; Masuda, S.; Dragnea, Y.; Moffat, K.; Bauer, C. E. *Biochemistry* **2006**, *45*, 12687.

(7) Jung, A.; Reinstein, J.; Domratcheva, T.; Shoeman, R. L.; Schlichting, I. *J. Mol. Biol.* **2006**, *362*, 717.

(8) Mataga, N.; Chosrowjan, H.; Shibata, Y.; Tanaka, F. *J. Phys. Chem. B* **1998**, *102*, 7081.

(9) Mataga, N.; Chosrowjan, H.; Shibata, Y.; Tanaka, F.; Nishina, Y.; Shiga, K. *J. Phys. Chem. B* **2000**, *104*, 10667.

(10) Mataga, N.; Chosrowjan, H.; Taniguchi, S.; Tanaka, F.; Kido, N.; Kitamura, M. *J. Phys. Chem. B* **2002**, *106*, 8917.

(11) Zhong, D.; Zwail, A. *Proc. Natl. Acad. Sci. U.S.A.* **2001**, *98*, 11867.

(12) Suto, K.; Kawagoe, K.; Shibata, N.; Morimoto, K.; Higuchi, Y.; Kitamura, M.; Nakaya, T.; Yasuoka, N. *Acta Crystallogr., Sect. D* **2000**, *56*, 368.

(13) Liepinsh, L.; Kitamura, M.; Murakami, T.; Nakaya, T.; Otting, G. *Nat. Struct. Biol.* **1997**, *4*, 975.

(14) Marcus, R. *J. Chem. Phys.* **1956**, *24*, 979.

(15) Moser, C.; Keske, J.; Warncke, K.; Farid, R.; Dutton, P. *Nature* **1992**, *355*, 796.

(16) Bixon, M.; Jortner, J. *J. Phys. Chem.* **1991**, *95*, 1941.

(17) Bixon, M.; Jortner, J.; Cortes, J.; Heitele, H.; Michel-Beyerle, M. E. *J. Phys. Chem.* **1994**, *98*, 7289.

(18) Kakitani, T.; Mataga, N. *J. Phys. Chem.* **1985**, *89*, 8.

(19) Kakitani, T.; Yoshimori, A.; Mataga, N. *J. Phys. Chem.* **1992**, *96*, 5385.

(20) Chosrowjan, H.; Taniguchi, S.; Mataga, N.; Tanaka, F.; Todoroki, D.; Kitamura, M. *J. Phys. Chem. B* **2007**, *111*, 8695.

(21) Chosrowjan, H.; Taniguchi, S.; Mataga, N.; Tanaka, F.; Todoroki, D.; Kitamura, M. *Chem. Phys. Lett.* **2008**, *462*, 121.

(22) Nunthaboot, N.; Tanaka, F.; Kokpol, S.; Chosrowjan, H.; Taniguchi, S.; Mataga, N. *J. Photochem. Photobiol. A* **2009**, *201*, 191.

(23) Nunthaboot, N.; Tanaka, F.; Kokpol, S.; Chosrowjan, H.; Taniguchi, S.; Mataga, N. *J. Phys. Chem. B* **2008**, *112*, 13121.

(24) Kitamura, M.; Kojima, S.; Ogasawara, K.; Nakaya, T.; Sagara, T.; Niki Miura, K.; Akutsu, H.; Kumagai, I. *J. Biol. Chem.* **1994**, *269*, 5566.

(25) Suto, K.; Kawagoe, K.; Shibata, N.; Morimoto, Y.; Higuchi, Y.; Kitamura, M.; Nakaya, T.; Yasuoka, N. *Acta Crystallogr.* **1999**, *D55*, 1089.

(26) Otwinowski, Z.; Minor, W. *Methods Enzymol.* **1997**, *276*, 307.

(27) Vagin, A.; Teplyakov, A. *Acta Crystallogr.* **2000**, *D56*, 1622.

(28) Brünger, A. T.; Adams, P. D.; Clore, G. M.; DeLano, W. L.; Gros, P.; Grosse-Kunstleve, R. W.; Jiang, J. S.; Kuszewski, J.; Nilges, M.; Pannu, N. S.; Read, R. J.; Rice, L. M.; Simonson, T.; Warren, G. L. *Acta Crystallogr.* **1998**, *D54*, 905.

(29) Emsley, P.; Cowtan, K. *Acta Crystallogr.* **2004**, *D60*, 2126.

(30) Murshudov, G. N.; Vagin, A. A.; Dodson, E. J. *Acta Crystallogr.* **1997**, *D53*, 240.

(31) Edmondson, D. E.; Tollin, G. *Biochemistry* **1971**, *10*, 124.

(32) Kitamura, M.; Terakawa, K.; Inoue, H.; Hayashida, T.; Suto, K.; Morimoto, Y.; Yasuoka, N.; Shibata, N.; Higuchi, Y. *J. Biochem.* **2007**, *141*, 459.

(33) Vorsa, V.; Kono, T.; Willey, K. F.; Winograd, L. *J. Phys.Chem. B* **1999**, *103*, 7889.

(34) Nunthaboot, N.; Tanaka, F.; Kokpol, K. *J. Photochem. Photobiol. A* **2009**, *207*, 274.

(35) Nunthaboot, N.; Tanaka, F.; Kokpol, K. *J. Photochem. Photobiol. A* **2010**, *209*, 70.

(36) Callis, P. R.; Liu, T. *Chem. Phys.* **2006**, *326*, 230.

JP912137S